



A Fault Ride-Through Technique for PMSG wind turbines using Superconducting Magnetic Energy Storage (SMES) under Grid voltage sag conditions.

Ernest F. Morgan¹, Tamer F. Megahed^{1,2}, Junya Suehiro³, Sobhy M. Abdelkader^{1,2}

¹Electrical Power Engineering, Egypt-Japan University of Science and Technology (E-JUST), New Borg El-Arab City, Alexandria 21934, Egypt

²Electrical Engineering Department, Faculty of Engineering, Mansoura University, El-Mansoura 35516, Egypt

³Faculty of Information Science and Electrical Engineering, Kyushu University, 744 Motoooka, Nishi-Ku, Fukuoka, 819-0395, Japan

* Corresponding Author:

Tel: (+20) 01025103144 / (+233) 240608086. e-mail: ernest.morgan@ejust.edu.eg

Abstract.

Wind power penetration is growing, posing considerable technological challenges for developing electrical grid systems. Gearless permanent magnet synchronous generator (PMSG) wind energy conversion systems (WECS) are becoming more popular. On the flip side, they are susceptible to grid failures. The use of Superconducting Magnetic Energy Storage (SMES) to enhance fault ride-through in PMSG wind turbines is investigated. Per the current Grid code trends, WECS are not to be disconnected from the grid; rather, they should provide reactive power support during such situations. This work incorporates machine and grid side converters to manage reactive, active power and DC-link voltage during grid failures. To improve system performance, lessen voltage dips at the point of common coupling (PCC), provide reactive power support and reduce the transient length, a DC-link capacitor is used with SMES. SMES reserve energy capacity is necessary for FRT operation when the wind turbine's inertial response range is insufficient. Finally, a 1.5 MW PMSG-based WTG with SMES is developed. The Pre-fault, fault-period, and post-fault performance are all assessed. They confirm the system's efficiency, speed, and stability.

Keywords: PMSGs, SMES, fault ride-through, wind energy, DC-link regulation.

1. Introduction.

Climate change resulting from global warming and ever-increasing energy consumption has escalated the use of renewable energy (RE) across the globe. COVID-19 restrictions implemented by nations have had little effect on renewable energy sources (RES) [1]. Renewable energy generation grew more than 3 % between January and March 2020 as compared to 2019 same period[2]. Admits covid the worldwide wind industry expanded by 53% in 2020, with a capacity of more than 93 GW, bringing the total global wind power capacity to 743 GW, with China and the United States being the world's

biggest markets [3]. WECS employing doubly-fed induction generators (DFIG), PMSGs, and squirrel cage induction generators (SCIG) have progressively been integrated into the electric grid in recent years [4]. The shutdown of wind power facilities would significantly impact the power system's transient and steady-state stability. E. ON, a German utility operator, implemented fault ride-through (FRT) standards in early 2003 to avoid the latter situation [5]. Direct drive wind turbines (WTs) seldom contribute to the fault current, which could meet FRT requirements. However, they will not enhance the system's voltage stability during grid outages. WECS should support the grid with reactive power to keep grid voltage stable [6]. As a result, FRT is critical for WTs in the event of grid faults. WTs should tolerate voltage fluctuations without being disconnected from the grid. PMSG and the WT are connected directly via a machine shaft. A back-to-back full-scale Voltage Source converter (VSC) and a transformer connect the stator winding of PMSG to the grid. Grid Side Converter (GSC) and machine side converter (MSC) are linked together by a DC-link capacitor [7]. This method has the benefits of great efficiency, no additional power source for field excitation is needed, and better reliability due to the absence of slip rings and gearbox [8]. When the PCC voltage declines owing to grid faults, the GSC current rises to keep the grid powered. The GSC current reaches its maximum with a high voltage drop, and power fed into the grid drops. Thus, a voltage drop at PCC will go unnoticed by the GSC controller since MSC continues to send real power via the DC-link capacitor. According to Babagharbani et al. [9] and Nasiri et al. [10], power imbalance rises the DC-link voltage and, if not properly managed, destroys the capacitor, which eventually damages the GSC and MSC. Hence, PMSG would not withstand significant voltage dips without protective hardware. Crowbar is the most well-known protection circuit-based method for isolating MSC [11]; it is linked across the rotor windings terminals and used only when there is a problem safeguarding the MSC by dissipating excess power using a DC

crowbar or DC chopper. Due to the crowbar's lower impedance as compared to the DC-link capacitor, Surplus power resulting from grid disturbance is routed to the crowbar and discarded [12]. The crowbar technique has several drawbacks, including the need for a huge resistor bank to dissipate MWs of power, a cooling system to disperse the heat produced by the crowbar, and the inability to meet grid code requirements [13]. A buck-boost converter connects an energy storage system (ESS) to the DC-link capacitor [14]. ESS absorbs the extra energy of the DC-link during a faulty event, preventing the DC-link from exceeding its voltage. After a problem has been cleared, the stored energy is sent to the grid network, improving the LVRT capabilities of the PMSG-based WECS. However, batteries have a slow discharge rate and less storage capacity.

To sum up, PMSGs are susceptible to Voltage Drop (VD) during faults. Still, new grid codes demand that they are not disconnected or shut down during such periods within an allowable time and should also provide reactive power support. For this reason, a strong FRT approach is required. A novel SMES-PMSG system is proposed in this work. SMES stores electricity and keeps the PCC's voltage constant. MSC and GSC are regulated to enhance power-sharing and SMES control to maintain PCC voltage and decrease transient duration. The system is tested under symmetrical grid voltage dip conditions. The suggested approach is less difficult and produces faster results.

The paper's contribution is summarized as follows.

- Proposed a novel hybrid energy system architecture based on PMSG and SMES.
- SMES control is designed to maintain PCC voltage, reduce transient time, and achieve FRT.

2. Power system model

The grid connected PMSG based wind power system considered in this study is depicted in Fig.1. It includes a wind turbine, a PMSG with a back-to-back converter, a grid side LC filter and three phase transmission lines.

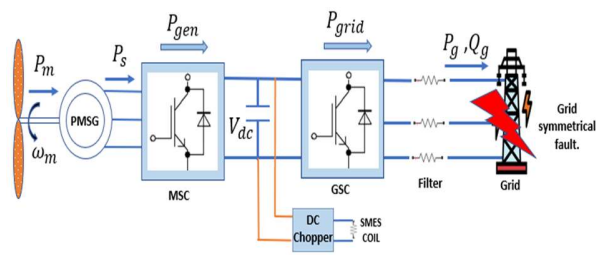


Figure 1: The basic topology of PMSG wind turbine system with SMES experiencing symmetrical voltage sags (dips).

2.1. FRT during grid symmetric voltage sag fault.

Vector control technique of GSC gives an output power as P_{gsc} [15].

$$P_{gsc} = \frac{3}{2} V_{gsc} i_{gscd} \quad (1)$$

Where P_{gsc} is the active power supplied to grid; i_{gscd} is the GSC d-axis current; V_{gsc} is the PCC voltage.

The dc-power links balance is [16].

$$\frac{1}{2} C \frac{dV_{dc}^2}{dt} = P_{msc} - P_{gsc} = \Delta P \quad (2)$$

where C represents capacitor capacitance; P_{msc} represents MSC output active power; V_{dc} represents dc voltage; ΔP stands for dc-link extra power. In the event of grid fault, the V_{gsc} will rapidly fall. According to equation (1), the P_{gsc} will start to decline when i_{gsc} reaches its limit due to the dip in PCC voltage. However, from equation (2), the dc voltage will excessively be raised, resulting in converter damage.

2.2. Machine side converter control.

MSC is a two-level voltage source converter (VSC) comprising six (6) IGBTs in a three-leg bridge configuration. As shown in Fig. 2, the cascaded control generates PWM to trigger the IGBTs. The MSC converts AC electricity to DC power.

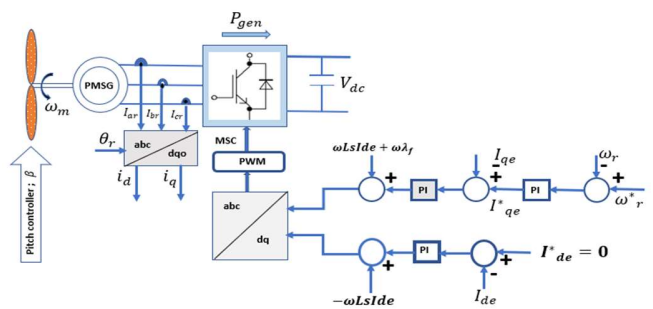


Figure 2: MSC control

2.3. Grid side converter control

The GSC is similar to the MSC, but it converts DC power to AC power. As illustrated in Fig. 3, the cascaded control generates the PWM. The phase-locked loop synchronizes the inverter and grid voltages.

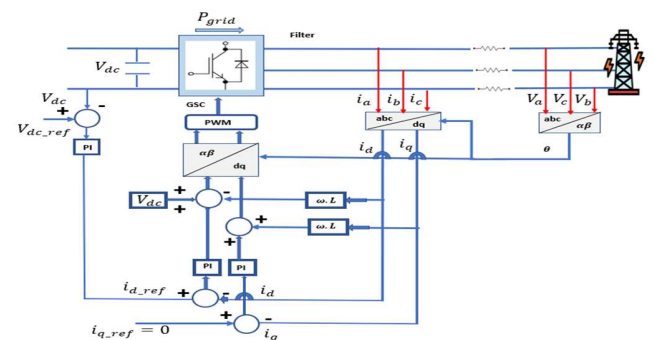


Figure 3: GSC control

2.4. DC-link and SMES model

The SMES coil is connected to the DC-link bus, as shown in Fig. 1. The SMES is linked to the DC/DC chopper converter

through a two-quarter IGBT-based DC/DC chopper converter to keep the DC-link voltage constant during transient faults. It may also act as a fault current limiter. The coil is bathed in helium to keep it cool and superconducting. Figure 4 shows a DC/DC chopper with two IGBTs and two diodes. A controller turns on the IGBTs during the charging condition. The IGBTs are turned off in the discharging condition, and the SMES discharges through the diodes. In the no-charge/discharge condition, a DC circulates between the coil, IGBTs, and diode.

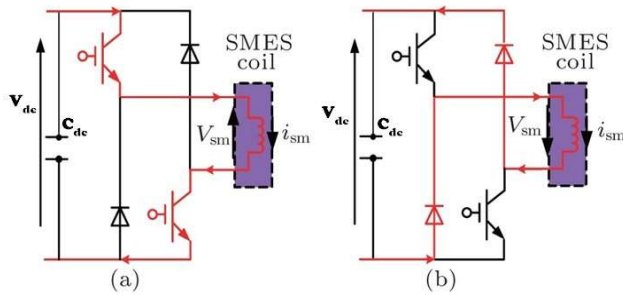


Figure 4: Operating modes of the SMES coil. (a) Charging, (b) Discharging

3. FRT control Method

In the suggested concept, energy held in SMES is automatically released to enhance system performance in grid fault situations. Thus, SMES reduces DC-link voltage fluctuations resulting from reduced active power during grid voltage symmetrical dips. A compensating voltage is promptly injected into the PMSG terminal to boost the FRT capabilities.

In the proposed control system depicted in Fig. 1, the voltage is stabilized by adjusting the SMES exchange power as follows:

- 1- After calculating the SMES power, the choice is made whether to charge or discharge SMES using switches, as illustrated in Fig. 4.
- 2- As illustrated in Fig. 5, the PI controller regulates the error signal and creates the duty cycle D , compared to a triangle signal with a frequency of 10 kHz.
- 3- The charging state happens when $D > 0.5$ and discharging state if $D < 0.5$. when $D = 0.5$, there is no charge or discharge, and that process is termed Idle state.

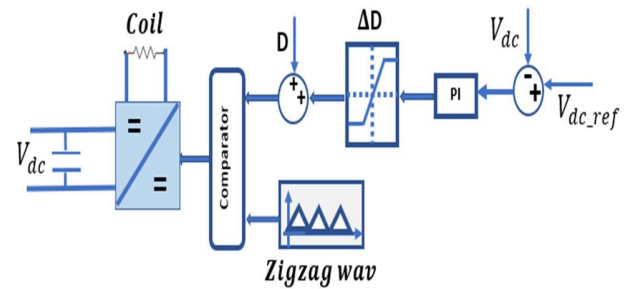


Figure 5: Schematic diagram of SMES controller

4. Case Study.

To test the suggested control strategy's efficacy, a 1.5 MW PMSG integrated with SMES is constructed. Table 1 shows some key parameters of SMES and PMSG. The voltage sag condition occurred between $t=4(s)$ and $t=5(s)$.

Table 1: System parameters

Rated power	1.5 MW	Voltage	575 V
Rated rotor voltage	1750 V	Frequency	60 Hz
Rated wind speed	12 m/s	DC-Voltage	1150 V
Inductance of SMES	10.73	Critical current of SMES	3375A

4.1. Faulty Condition.

Fig. (5) depicts the impact of voltage sag on PMSG WECS. Fig. 5(a) depicts a 90% decline in grid voltage, which substantially impacts grid power quality. The grid-connected current shown in Fig. 5 (b) of the PMSG WECS is prolonged beyond the fault period causing active power Fig. 5 (c) and reactive power Fig 5 (d) to be absorbed by the WECS at rates of 1.2 MW and 0.07Mvar, respectively. In addition, Fig 5 (e) depicts the DC-link voltage imbalance caused by substantial changes in the GSC's input and output power; when Dc link capacitor voltage exceeds the 2300V mark, the machine without protection will be forced to shut down.

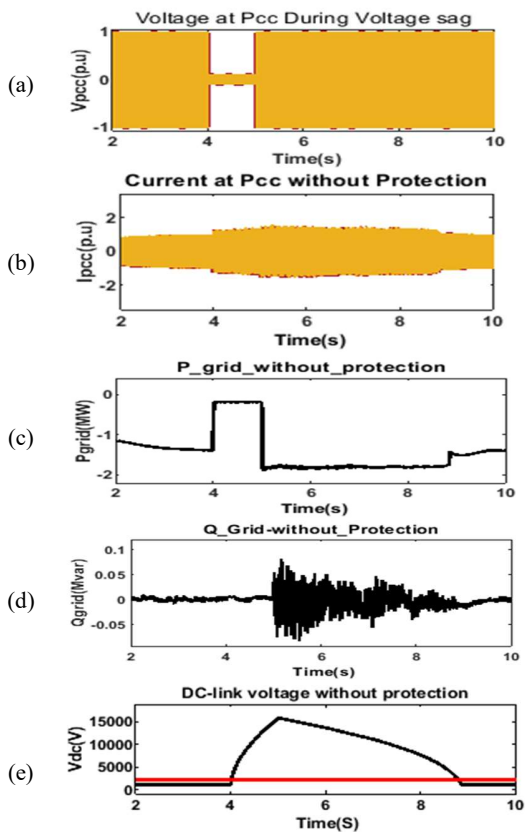


Figure 5(a-e): Shows the performance of PMSG wind turbine during grid voltage sag conditions without protection.

4.2 LVRT of the Wind Power System

As illustrated in Fig. 6(a), the suggested control approach limits the grid-connected current to the maximum permitted time frame equal to the voltage sag condition. As demonstrated in Fig. 6(b & c), the wind turbine and generator-side converter both retain regular functioning throughout the dip, allowing the generator's output power to remain almost constant. The grids average active power intake declines from 1.5 to 0.18 MW (shown in Figure 6(b)), and with the help of SMES steadily after the fault clearing time, active power is being restored to its rated 1.5MW, and reactive power in Figure 6(c) is kept steadily close to 0 Mvar to prevent any reverse flow of power. Without SMES, the DC-link voltage rises fast, threatening the regular functioning of the PMSG WECS. Fig. 6(d) shows how the bi-directional DC-DC chopper controls the collected power in the DC bus so that the SMES can absorb it and keep the DC bus voltage within an operatable range. Meanwhile, the current charge of SMES during the said condition is shown in Figure 6(e).

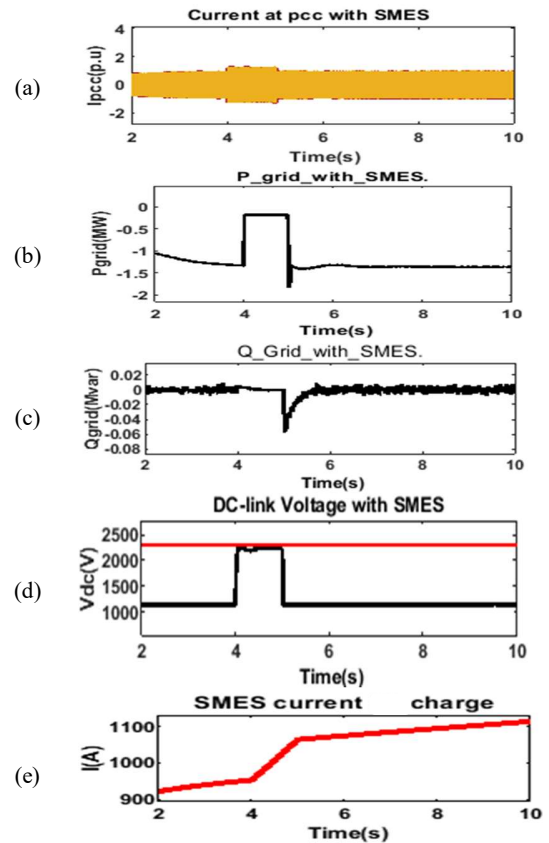


Figure 6(a-e): Shows the performance of PMSG wind turbine during grid voltage sag conditions with the proposed protection scheme.

5. Conclusion

A new combination scheme based on SMES for improving the FRT capability of PMSG has been proposed and validated. The fundamental idea, system topology, control method, simulation verification, and performance assessment have been completed. The simulation results verifies that the proposed SMES device can support PCC active power and sustain dc-link voltage during grid disturbances. Thus, the suggested FRT approach improves the FRT capability of the PMSG system.

Reference

- [1] A. Naderipour *et al.*, "Effect of COVID-19 virus on reducing GHG emission and increasing energy generated by renewable energy sources: A brief study in Malaysian context," *Environ. Technol. Innov.*, vol. 20, p. 101151, Nov. 2020, doi: 10.1016/J.ETI.2020.101151.
- [2] M. Khanna, "COVID-19: A Cloud with a Silver Lining for Renewable Energy?," *Appl. Econ. Perspect. Policy*, vol. 43, no. 1, pp. 73–85, Mar. 2021, doi: 10.1002/AEPP.13102.
- [3] P. Jiang, Y. Van Fan, and J. J. Klemeš, "Impacts of COVID-19 on energy demand and consumption: Challenges, lessons and emerging opportunities," *Appl. Energy*, vol. 285, p. 116441, Mar. 2021, doi: 10.1016/J.APENERGY.2021.116441.
- [4] O. P. Mahela, N. Gupta, M. Khosravy, and N. Patel, "Comprehensive overview of low voltage ride through methods of grid integrated wind generator," *IEEE Access*, vol. 7, pp. 99299–99326, 2019, doi: 10.1109/ACCESS.2019.2930413.
- [5] D. Flynn *et al.*, "Technical impacts of high penetration levels of wind power on power system stability," *Wiley Interdiscip. Rev. Energy Environ.*, vol. 6, no. 2, p. e216, Mar. 2017, doi: 10.1002/WENE.216.
- [6] Y. L. Hu, Y. K. Wu, C. K. Chen, C. H. Wang, W. T. Chen, and L. Il Cho, "A Review of the Low-Voltage Ride-Through Capability of Wind Power Generators," *Energy Procedia*, vol. 141, pp. 378–382, Dec. 2017, doi: 10.1016/J.EGYPRO.2017.11.046.
- [7] M. Deepu Vijay, B. Singh, and gurumoorthy Bhuvanewari, "Sensorless SynRG Based Variable Speed Wind Generator and Single-Stage Solar PV Array Integrated Grid System with Maximum Power Extraction Capability," *IEEE Trans. Ind. Electron.*, vol. 67, no. 9, pp. 7529–7539, Sep. 2020, doi: 10.1109/TIE.2019.2942511.
- [8] D. P. Aguemon, R. G. Agbokpanzo, F. Dubas, A. Vianou, D. Chamagne, and C. Espanet, "A Comprehensive Analysis and Review on Electrical Machines in Wind Energy Conversion Systems," *Adv. Eng. Forum*, vol. 35, pp. 77–93, Feb. 2020, doi: 10.4028/WWW.SCIENTIFIC.NET/AEF.35.77.
- [9] B. Babaghorbani, M. T. Beheshti, and H. A. Talebi, "A Lyapunov-based model predictive control strategy in a permanent magnet synchronous generator wind turbine," *Int. J. Electr. Power Energy Syst.*, vol. 130, no. January, p. 106972, 2021, doi: 10.1016/j.ijepes.2021.106972.
- [10] M. Nasiri, A. Arzani, and M. Savaghebi, "Current limitation for the machine side converter of permanent magnet synchronous generator wind turbines during grid faults," *IET Renew. Power Gener.*, vol. 14, no. 17, pp. 3448–3456, Dec. 2020, doi: 10.1049/IET-RPG.2019.1246.
- [11] P. Han, M. Cheng, S. Ademi, and M. G. Jovanović, "Brushless doubly-fed machines: Opportunities and challenges," *Chinese J. Electr. Eng.*, vol. 4, no. 2, pp. 1–17, Jun. 2018, doi: 10.23919/CJEE.2018.8409345.
- [12] O. Noureldeen and I. Hamdan, "Design and Analysis of Combined Chopper-Crowbar Protection Scheme for Wind Power System Based on Artificial Intelligence," *2018 20th Int. Middle East Power Syst. Conf. MEPCON 2018 - Proc.*, pp. 809–814, Feb. 2019, doi: 10.1109/MEPCON.2018.8635177.
- [13] S. Ali, E. E. Elkholy, H. Hegazy, and H. Awad, "Comparison between Hardware and Programming Solutions to Alleviate Influence of Voltage Dips on Wind Energy Systems," *2021 22nd Int. Middle East Power Syst. Conf.*, pp. 45–50, Dec. 2021, doi: 10.1109/MEPCON50283.2021.9686216.
- [14] K. K. Pandey *et al.*, "Bidirectional DC-DC Buck-Boost Converter for Battery Energy Storage System and PV Panel," *Smart Innov. Syst. Technol.*, vol. 206, pp. 681–693, 2021, doi: 10.1007/978-981-15-9829-6_54.
- [15] R. Vijaya Priya and R. Elavarasi, "Vector Control Scheme for the PMSG-Based WPS Under Various Grid Disturbances," *Lect. Notes Electr. Eng.*, vol. 688, pp. 303–319, 2021, doi: 10.1007/978-981-15-7241-8_22.
- [16] J. X. Jin, R. H. Yang, R. T. Zhang, Y. J. Fan, Q. Xie, and X. Y. Chen, "Combined low voltage ride through and power smoothing control for DFIG/PMSG hybrid wind energy conversion system employing a SMES-based AC-DC unified power quality conditioner," *Int. J. Electr. Power Energy Syst.*, vol. 128, p. 106733, Jun. 2021, doi: 10.1016/J.IJEPES.2020.106733.